1 **Designing laboratory metallic iron columns for better result comparability**

2 Noubactep C.[*(a,c)], Caré S.[(b)]

3 [(a)] Angewandte Geologie, Universität Göttingen, Goldschmidtstraße 3, D - 37077 Göttingen, Germany;

4 [(b)] Université Paris-Est, Laboratoire Navier, (ENPC/IFSTTAR/CNRS), 2 allée Kepler, 77420 Champs sur Marne,

5 France;

6 [(c)] Kultur und Nachhaltige Entwicklung CDD e.V., Postfach 1502, D - 37005 Göttingen, Germany.

7 * corresponding author: e-mail: cnoubac@gwdg.de; Tel. +49 551 39 3191, Fax: +49 551 399379

8 **Abstract**

9 Despite the amount of data available on investigating the process of aqueous contaminant

10 removal by metallic iron (Fe^0), there is still a significant amount of uncertainty surrounding

11 the design of Fe^0 beds for laboratory testing to determine the suitability of Fe^0 materials for

12 field applications. Available data were obtained under various operating conditions (e.g.

13 column characteristics, Fe^0 characteristics, contaminant characteristics, oxygen availability,

14 solution pH) and are hardly comparable to each other. The volumetric expansive nature of

15 iron corrosion has been univocally reported as major drawback for Fe^0 beds. Mixing Fe^0 with

16 inert materials has been discussed as an efficient tool to improve sustainability of Fe^0 beds.

17 This paper discusses some problems associated with the design of Fe^0 beds and proposes a

18 general approach for the characterization of Fe^0 beds. Each Fe^0 column should be

19 characterized by its initial porosity, the composition of the steady phase and the volumetric

20 proportion of individual materials. Used materials should be characterized by their density,

21 porosity, and particle size. This work has introduced simple and reliable mathematical

22 equations for column design, which include the normalisation of raw experimental data prior

23 to any data treatment.

24 **Key words**: Deep bed filtration, Operational parameters, Results comparability, Water

25 Filtration; Zerovalent iron.

26

1 **Introduction**

Metallic iron (Fe^0) as reactive medium for aqueous contaminant removal has been intensively investigated during the last two decades [1-6]. These studies have demonstrated the potential of Fe^0 for use in (i) subsurface permeable reactive barriers [1], (ii) above ground wastewater treatment [3,5], (iii) household water filters [7-10], and (iv) drinking water treatment plants [11-13]. The fundamental mechanisms of contaminant removal in Fe^0 beds are adsorptive size-exclusion and co-precipitation [5,6,13-19].

Data for pilot- and full-scale remediation scheme are mostly obtained from laboratory columns [20-22]. Laboratory column studies are in turn conventionally designed based on batch treatability studies [21,23,24]. A major problem of available data from batch studies is the poor comparability of results from different laboratories using different conditions. Most experimental conditions are not relevant for field situations [25,26]. For example, only shaking intensity lower than 50 m^{-1} could enable the formation of a universal oxide-scale in the vicinity of the Fe^0 surface as observed in column studies and in full-scale barriers [25]. A careful look behind published data on laboratory column experiments ([27-32]; see Tab. 1) also demonstrates large variability in the experimental design. General design procedures are not available. Differences in design procedures may cloud interpretations of reported data. Therefore, any effort to ensure the comparability of laboratory results over time and space would accelerate the development of the Fe^0 remediation technology.

The objective of the present communication is to improve the comparability of laboratory column results by offering the scientific community tools for a common basis for the design of Fe^0 beds. Previous theoretical works [9,31,32] have demonstrated that mixing Fe^0 and other materials (gravel, pumice, sand, quartz) is the prerequisite for long service life. This mixture should be characterized by the volumetric proportion of Fe^0 (Fig. 1) and other materials (additives) and the initial porosity [32]. The specific objective of this communication is to establish equations for the evaluation of the mass of the materials to be used.

2   Basis for comparable results

Cylindrical columns usually used for laboratory experiments primarily differ in their size (diameter * length). For example, columns with 5 cm internal diameters exist with lengths varying from 30 to 100 cm (Tab. 1). Completely filling the six different columns from Tab. 1 with reactive materials (e.g. Fe^0) will yield 0.2 to 9.8 kg of Fe^0 for the experiment. The question is how to objectively compare results obtained with various amount of the same materials? The situation is exacerbated when the materials are different (particle size, shape, chemical composition or generally intrinsic reactivity). When material mixture should be performed, the rationale for purposeful mixing should be developed.

Using the material apparent specific weight tabulated by Noubactep and Caré [9], Tab. 1 clearly shows that a given volume (e.g. V_{solid} in the same column) is occupied by a mass m of pumice, 4.14*m of sand, and 12.19*m of Fe^0. The coefficients are the ratios of the apparent specific weights (ρ_i/ρ_j). This observation confirms that the volumetric ratio is the sole appropriate approach to design column studies. Accordingly, an approach to have comparable results could be to fix the Fe^0 volume. A given Fe^0 volume corresponds to various heights depending on the column internal diameter. Accordingly, beside used Fe^0 mass (corresponding to a volumetric fraction of solid), the column dimensions should always be specified. Three examples are given below for illustration.

In the laboratory, the Fe^0 amount is commonly given in weight (g or kg). Therefore, a practical approach is to fix a mass of Fe^0 (m_0) which is likely to enable observable effects within a reasonable time (e.g. 6 weeks).

- An experiment is designed to compare the reactivity of different Fe^0 materials. Parallel column experiments have to be conducted in which Fe^0 is the sole variable and the same mass (m_0) is used in individual columns.

- An experiment is designed to compare the impacts of chloride (Cl^-) and sulphates (SO_4^{2-}) on the efficient of a Fe^0 for methylene blue (MB) discoloration. The three following parallel

3

78   experiments could be conducted with the mass m_0 of a Fe^0 sample: (i) MB in deionised water,

79   (ii) MB in a Cl^- solution, and (iii) MB in a SO_4^{2-} solution. The MB concentration is the same

80   in all experiments, Cl^- and SO_4^{2-} solutions have the same equivalent concentration.

81   - An experiment is designed to compare the impact of mixing Fe^0 with additives. The

82   reference system should be the mass m_0 of Fe^0, and volumetric proportions of Fe^0 have to be

83   replaced by appropriated additives. Tab. 1 shows that each column is characterized by a

84   constant pore volume which is the external or inter-granular porosity. For porous materials the

85   internal porosity or intra-granular porosity has been discussed as a storage room for in-situ

86   generated corrosion products and thus a tool to sustain Fe^0 reactivity [9,10,32]. Similarly,

87   mixing Fe^0 and non-porous inert additives is beneficial for the system because inert material

88   will not contribute to pore filling or filter clogging.

89   The next section will establish some general equations to support design operations.

90   **3   Mathematical equations for column design**

91   A hypothetical cylindrical filter having an inner diameter D, a length L, and a reactive zone

92   h_{rz} is considered. The reactive zone is the fraction of L ($L > h_{rz}$) containing the reactive

93   material, possibly mixed with selected additives. The filter is filled by spherical particles

94   (reactive materials and non-reactive additives) having a constant diameter d. Considering the

95   granular material as composed of mono-dispersed spheres subjected to soft vibrations, the

96   column compactness (or packing density) C ranges between 0.60 and 0.64 for a random close

97   packing but it is generally considered to be equal to 0.64 (limit value). It can be noticed that

98   the value of the compactness depends on various parameters as the distribution size of

99   particles, their shape [33-34]. The theoretical value of C = 0.64 is strictly valid for particles

100 with spherical shape and similar sizes. It is assumed in this study that ratio of cylinder

101 diameter (D = 2*R) to particle diameter (d), $\beta = 2*R/d$ is optimal for axial hydrodynamic

102 dispersion [36,37].

103 The volume of the reactive zone (V_{rz}), the volume of solid (V_{solid}), the volume of inter-

104 granular pores (V_{pore}), the volume of individual solids (V_i) with the apparent specific weight

105 ρ_i, and the thickness of the reactive zone (h_{rz}) are given by Eq. 1 through Eq. 6:

$$V_{rz} = \pi * D^2 * h_{rz}/4 \qquad (1)$$

$$V_{rz} = V_{solid} + V_{pore} \qquad (2)$$

$$V_{solid} = C * V_{rz} \qquad (3a)$$

$$V_{pore} = (1 - C) * V_{rz} \qquad (3b)$$

$$V_{solid} = \Sigma V_i = V_{solid1} + V_{solid2} + V_{solid3} + \dots \qquad (4)$$

$$V_i = m_i/\rho_i \qquad (5)$$

$$h_{rz} = 4V_{rz}/\pi * D^2 = 4V_{solid}/(C * \pi * D^2) \qquad (6)$$

3.1 Volumetric solid fractions in the reactive zone

114 Replacing V_{solid} in Eq. 2 by its expression from Eq. 4 yields:

$$V_{rz} = V_{solid} + V_{pore} = V_{pore} + \Sigma V_i \Rightarrow \alpha_{pore} + \Sigma\alpha_i = 1 \qquad (7)$$

116 where α_{pore} and α_i are the volumetric fractions of the inter-granular pores and of the individual

117 solid phase "i" in the column respectively. The fractions are related to the volume of the

118 reactive zone V_{rz}.($\alpha_{pore} = V_{pore}/V_{rz}$ and $\alpha_i = V_{solid\,i}/V_{rz}$).

119 Eq. 7 suggests that $\Sigma\alpha_i$ is necessarily equal to C. Thus, Eq. 2 should be written:

$$V_{rz} = V_{solid} + V_{pore} = V_{rz} (\alpha_{pore} + \Sigma\alpha_i) \qquad (8)$$

121 For instance, for a system containing a mixture of four solid phases, Eq. 7 should read:

$$\alpha_{pore} + \alpha_1 + \alpha_2 + \alpha_3 + \alpha_4 = 1 \qquad (8a)$$

123 or $\qquad \alpha_1 + \alpha_2 + \alpha_3 + \alpha_4 = 1 - \alpha_{pore} = C \qquad (8b)$

124 Eq. 8 is very important for the calculations of the amounts of individual additives to achieve

125 wished material mixtures as will be discussed in the next section. Eq. 8b suggests that α_i is

126 necessarily a fraction of C. Thus, a simple rule of proportion can be established to calculate α_i

127   for each proportion P_i of the solid phase. C necessarily corresponds to 100 % solid. The

128   relation between α_i and P_i is given by Eq. 9:

129                 $\alpha_i = C*P_i/100$ (9)

130   Tab. 2 gives some values of α_i for selected relevant P_i values. For example, if a quaternary

131   system should be made up of 40 % of material A, 30 % material B, 20 % material C and 10 %

132   material D, the coefficients to be used are: 0.256, 0.192, 0.128 and 0.064 respectively. A

133   quaternary system seems to be strange or complicated. However, such a system could

134   comprise Fe^0 as basic reactive material, MnO_2 to sustain Fe^0 reactivity, pumice as storage

135   solid and quartz as non-porous inert filling material.

136   **3.2   Initial porosity of reactive the zone**

137   In the case of non porous spherical particles, the initial porosity of the reactive zone Φ_0 is the

138   inter-granular porosity α_{pore} and is given by Eq. 10 [32].

139                 $\Phi_0 = 1 - C$ (10)

140   If individual particles are porous, the intra-granular porosity should be considered [32]. In this

141   case the initial porosity should read:

142                 $\Phi_0 = (1 - C) + \Sigma\alpha_i\phi_i$ (11)

143   where C is the compactness of the reactive zone, α_i the volumetric fraction of the solid i (Tab.

144   2) and ϕ_i its internal porosity.

145   Equations 1 to 11 are the basis for purposeful experimental design as will be discussed below

146   for selected cases.

147   **4   Designing some Fe^0 systems**

148   **4.1   A four component system**

149   For the design of a quaternary system of Fe^0, sand, pumice and MnO_2, Eq. 8 can be used:

150                 $V_{rz} = V_{rz} (\alpha_{pore} + \alpha_{Fe} + \alpha_{sand} + \alpha_{pumice} + \alpha_{MnO2})$

151                 $V_{rz} = \alpha_{pore}* V_{rz} + \alpha_{Fe}*V_{rz} + \alpha_{sand}*V_{rz} + \alpha_{pumice}*V_{rz} + \alpha_{MnO2}* V_{rz}$

152 $$V_{rz} = V_{pore} + V_{Fe} + V_{sand} + V_{pumice} + V_{MnO2}$$

153 Assuming $V_{rz} = 1000$ mL, $\alpha_{Fe} = 0.192$ ($P_{Fe} = 30$ %), $\alpha_{sand} = 0.256$ ($P_{sand} = 40$ %), $\alpha_{pumice} =$

154 0.128 ($P_{pumice} = 20$ %), and $\alpha_{MnO2} = 0.064$ ($P_{MnO2} = 10$ %), the volume of the materials are

155 192, 256, 128 and 64 mL respectively and $V_{pore} = 360$ mL.

156 Using Eq. 5 ($m_i = \rho_i * V_i$), the needed mass of each material can be calculated. Results showed

157 that 1498 g of Fe, 678 g of sand, 82 g of pumice and 224 g of MnO_2 will be used and

158 homogeneously mixed to design the desired column.

159 The initial porosity of the resulted column is given by Eq. 11

160 $$\Phi_0 = (1 - C) + \alpha_{Fe}\phi_{Fe} + \alpha_{sand}\phi_{sand} + \alpha_{pumice}\phi_{pumice} + \alpha_{MnO2}\phi_{MnO2}$$

161 But Fe and sand (quartz) are non-porous, therefore Φ_0 is given by:

162 $$\Phi_0 = (1 - C) + \alpha_{pumice}\phi_{pumice} + \alpha_{MnO2}\phi_{MnO2}$$

163 Using values above ($\alpha_{pumice} = 0.128$ and $\alpha_{MnO2} = 0.064$), $\phi = 0.80$ (80 %) for pumice, and $\phi =$

164 0.25 (25 %) for MnO_2, give an initial porosity of 0.48 (vs. 0.36 in a pure Fe^0 column).

165 This example shows an increase of the initial porosity by 33 % for the given mixture.

166 **4.2 Working with a constant Fe^0 mass**

167 To work with a constant Fe^0 mass, the volume (V_{Fe}) occupied by the given Fe mass is

168 calculated using Eq. 5. This volume represents a certain fraction of solid in the filter (α_{Fe} in

169 Eq. 8a). Knowing V_{solid}, the volume of the reactive zone V_{rz} and its thickness h_{rz} can be

170 deduced using Eq. 3c and Eq. 6.

171 It is obvious, that h_{rz} depends on the inner diameter of the filter. Accordingly, the simplest

172 way to investigate the effect of bed thickness on the efficiency of Fe^0 beds is to work with a

173 constant Fe^0 mass, representing a fix volumetric percentage of solid and using columns of

174 various internal diameters (D_i).

175 Working with a constant Fe^0 mass can be regarded as the most powerful tool to achieve

176 comparable results. For example, laboratory column experiments could be routinely

177 performed with 100 g of Fe^0 representing 30 vol-% of the solid in the reactive zone.

178 Calculations show that the reactive zone will occupy a volume of 20 mL. To have such a

179 volume using columns with inner diameters D_1 (2.0 cm), D_2 (2.6 cm) and D_3 (5.0 cm), the

180 column length should be 6.37, 3.77, and 1.02 cm respectively. All columns of Tab. 1 satisfy

181 this basic condition. However building an homogeneous 1.02 cm layer of "Fe^0 + additive"

182 could be a difficult task. While repeating the calculations above with 250 g Fe^0 results show

183 that needed column lengths are 15.93, 9.43, and 2.55 cm respectively. While column 1 (D = 2

184 cm, L = 12 cm) is no more applicable, filling column 3 (D = 5 cm) with only 2.55 cm of

185 homogeneous mixture could still be difficult to achieved. Therefore and objective could be a

186 minimum reactive zone length of 5 cm. To achieve this thickness, a Fe^0 of 500 g is needed for

187 column 3. This is necessarily coupled with longer experimental duration. As a result, it is

188 suggested that columns with more than 3 cm internal diameter are not suitable for short term

189 laboratory experiments. This suggestion is coupled with the desire to save Fe^0 costs in

190 columns and to shorten experimental durations.

191 **4.3   Working with a constant initial porosity**

192 For column experiments performed with a constant Fe^0 mass (e.g. 100 g), using various

193 additives could enable a constant initial porosity (Φ_0). The aim could be for example to

194 experimentally quantify the impact of MnO_2 on Fe^0 bed's hydraulic permeability. The length

195 of the reactive zone will vary as a function of the porosity of the tested additive. Eq. 11 (Φ_0 =

196 $(1 - C) + \Sigma\alpha_i\phi_i$) should be solved while fixing one or two variables.

197 For example, the reference system uses Fe^0 (100 g representing 50 vol-%) and a limestone

198 with ϕ_{lime} = 25 %. A second system having the same initial porosity (Φ_0) and been made up of

199 Fe (ϕ_{Fe} = 0 %), quartz (ϕ_{quartz} = 0 %) and pumice should be designed. Which pumice amount

200 should be used?

201   For the reference system, $\alpha_{Fe} = 0.32$; $\phi_{Fe} = 0$; $\alpha_{lime} = 0.32$; and $\phi_{lime} = 0.25$. Calculations give

202      $\Phi_0 = 1 - C + 0.32*0.25 = 0.44$. Now, Eq. 11 ($\Phi_0 = 0.44$) should be written for the unknown

203   system and solved for ϕ_{pumice}, given $\alpha_{Fe} = 0.32$ (or $\alpha_{quartz} + \alpha_{pumice} = 0.32$). That is, with $\phi_{Fe} =$

204      $\phi_{quartz} = 0$:

205 $$\Phi_0 = 0.44 = 1 - C + \alpha_{Fe}\phi_{Fe} + \alpha_{quartz}\phi_{quartz} + \alpha_{pumice}\phi_{pumice} \qquad (11a)$$

206 $$\alpha_{pumice} = 0.08/\phi_{pumice} \qquad (11b)$$

207   The pumices to be used are materials for which Eq. 11b and the fundamental conditions α_{quartz}

208      $+ \alpha_{pumice} = 0.32$ and $\phi_{pumice} < 0.9$ are respected. There are certainly a large number of possible

209   solutions but the appropriate solution will be dictated by pumice's availability. Table 3

210   summarizes 5 appropriate solutions corresponding to ϕ_{pumice} values varying from 0.33 to 0.80.

211   Having the α_{pumice} (and α_{quartz}) the volumes and the masses can be derived and used as

212   described above.

213   **5   Concluding remarks**

214   To date, the equivocal results published on contaminant removal in Fe^0/H_2O systems

215   demonstrate that the physico-chemical mechanisms of the remediation process still remain

216   unclear [38]. Available data were produced and interpreted based on the concept that Fe^0 is a

217   reducing agent [1-4]. On the other side, available data are characterized by the diversity of

218   experimental conditions under which they are obtained (Tab. 1). This situation is not

219   favourable for reliable data comparison. In particular, further laboratory column studies

220   aiming at optimising field Fe^0 bed design efforts should be acquired under reproducible

221   experimental conditions.

222   The present theoretical study has initiated a new path to an harmonized experimental protocol

223   for column experiments. It is proposed that 100 g or 250 g of Fe^0 is used in a volumetric

224   proportion not larger than 50 %. The equations for material mixtures are established. It is

225   hoped that researchers will use the developed tools to avoid inconsistent results which are

most likely the product of inaccurate experimental designs. For example, while bed clogging

has been reported as the major drawback of the Fe^0 technology, most researchers have used

experimental designs favouring column clogging ($Fe^0 > 60$ vol-%) [32].

Once the mass of Fe^0 and its volumetric proportion are fixed several other factors can be

purposefully discussed. For example, the impact of: (i) the Fe^0 average particle size, (ii) the

solution pH, (iii) the water composition, (iv) water flow velocity. In all the case the

description of the experimental protocol should include and extensive description of used

materials (density, porosity, measured bed porosity). Finally, because clogging is the major

problem of Fe^0 beds, expertise from other branches of environmental science dealing with

porous media clogging could be helpful for proper Fe^0 bed design. In particular, much

impetus could come from the impact of bio-clogging on the evolution of the porosity of

constructed wetland [39-42].

References

[1] S.F. O´Hannesin, R.W. Gillham, Long-term performance of an in situ "iron wall" for
     remediation of VOCs, Ground Water 36 (1998) 164–170.

[2] A.D. Henderson, A.H. Demond, Long-term performance of zero-valent iron permeable
     reactive barriers: a critical review, Environ. Eng. Sci. 24 (2007) 401–423.

[3] A.B. Cundy, L. Hopkinson, R.L.D. Whitby, Use of iron-based technologies in
     contaminated land and groundwater remediation: A review, Sci. Tot. Environ. 400
     (2008) 42–51.

[4] R. Thiruvenkatachari, S. Vigneswaran, R. Naidu, Permeable reactive barrier for
     groundwater remediation, J. Ind. Eng. Chem. 14 (2008) 145–156.

[5] A. Ghauch, H.A. Assi, A. Tuqan, Investigating the mechanism of clofibric acid removal in
     Fe^0/H_2O systems, J. Hazard. Mater. 176 (2010) 48–55.

[6] A. Ghauch, H.A. Assi, S. Bdeir, Aqueous removal of diclofenac by plated elemental iron:
     Bimetallic systems, J. Hazard. Mater. 182 (2010) 64–74.

252   [7] C. Noubactep, A. Schöner, P. Woafo, Metallic iron filters for universal access to safe

253   drinking water, Clean: Soil, Air, Water 37 (2009) 930–937.

254   [8] M.I. Litter, M.E. Morgada, J. Bundschuh, Possible treatments for arsenic removal in Latin

255   American waters for human consumption, Environ. Pollut. 158 (2010) 1105–1118.

256   [9] C. Noubactep, S. Caré, Enhancing sustainability of household water filters by mixing

257   metallic iron with porous materials, Chem. Eng. J. 162 (2010) 635–642.

258   [10] C. Noubactep, S. Caré, Dimensioning metallic iron beds for efficient contaminant

259   removal, Chem. Eng. J. 163 (2010) 454–460

260   [11] A.M. Gottinger, D.J. Wild, D. McMartin, B. Moldovan,. D. Wang, Development of an

261   iron-amended biofilter for removal of arsenic from rural Canadian prairie potable water,

262   In: Water Pollution X. A.M. Marinov and C.A. Brebbia, Eds.; WIT Press: Ashurst,

263   Southampton (2010) 333–344.

264   [12] C. Noubactep, A. Schöner, Metallic iron: dawn of a new era of drinking water treatment

265   research? Fresen. Environ. Bull. 19 (2010) 1661–1668.

266   [13] C. Noubactep, Metallic iron for safe drinking water worldwide, Chem. Eng. J. 165

267   (2010) 740–749

268   [14] C. Noubactep, Processes of contaminant removal in "Fe^0-H_2O" systems revisited. The

269   importance of co-precipitation, Open Environ. J. 1 (2007) 9–13.

270   [15] C. Noubactep, A critical review on the mechanism of contaminant removal in Fe^0-H_2O

271   systems, Environ. Technol. 29 (2008) 909–920.

272   [16] C. Noubactep, An analysis of the evolution of reactive species in Fe^0/H_2O systems, J.

273   Hazard. Mater. 168 (2009) 1626–1631.

274   [17] C. Noubactep, Elemental metals for environmental remediation: Learning from

275   cementation process, J. Hazard. Mater. 181 (2010) 1170–1174.

276   [18] C. Noubactep, The fundamental mechanism of aqueous contaminant removal by metallic

277   iron, Water SA 36 (2010) 663–670.

278 [19] C. Noubactep, The suitability of metallic iron for environmental remediation, Environ.

279   Progr. Sust. En. 29 (2010) 286–291.

280 [20] J.O. Peterson, G.F. Lee, Sorption capacity estimation for activated carbon packed

281   columns, Water Res. 5 (1971) 717–721.

282 [21] C. Su, R.W. Puls, In situ remediation of arsenic in simulated groundwater using

283   zerovalent iron: Laboratory column tests on combined effects of phosphate and silicate,

284   Environ. Sci. Technol. 37 (2003) 2582–2587.

285 [22] S. Kundu, A.K. Gupta, Analysis and modeling of fixed bed column operations on As(V)

286   removal by adsorption onto iron oxide-coated cement (IOCC), J. Colloid Interf. Sci. 290

287   (2005) 52–60.

288 [23] K.L. McGeough, R.M. Kalin, P. Myles, Carbon disulfide removal by zero valent iron,

289   Environ. Sci. Technol. 41 (2007) 4607–4612.

290 [24] T.-H. Wang, M.-H. Li, S.-P. Teng, Bridging the gap between batch and column

291   experiments: A case study of Cs adsorption on granite, J. Hazard. Mater. 161 (2009)

292   409–415.

293 [25] C. Noubactep, A.-M.F. Kurth, M. Sauter, Evaluation of the effects of shaking intensity

294   on the process of methylene blue discoloration by metallic iron, J. Hazard. Mater. 169

295   (2009) 1005–1011.

296 [26] C. Noubactep, T. Licha, T.B. Scott, M. Fall, M. Sauter, Exploring the influence of

297   operational parameters on the reactivity of elemental iron materials, J. Hazard. Mater.

298   172 (2009) 943–951.

299 [27] M. Gheju, I. Balcu, Hexavalent chromium reduction with scrap iron in continuous-flow

300   system. Part 2: Effect of scrap iron shape and size, J. Hazard. Mater. 182 (2010) 484–

301   493.

302 [28] C. Noubactep, Characterizing the reactivity of metallic iron in Fe^0/EDTA/H_2O systems

303   with column experiments, Chem. Eng. J. 162 (2010) 656–661.

304   [29] A. Luna-Velasco, R. Sierra-Alvarez, B. Castro, J.A. Field, Removal of nitrate and

305   hexavalent uranium from groundwater by sequential treatment in bioreactors packed

306   with elemental sulfur and zero-valent iron, Biotechnol. Bioeng. 107 (2010) 933–942.

307   [30] P. Westerhoff, J. James, Nitrate removal in zero-valent iron packed columns, Wat. Res.

308   37 (2003) 1818–1830.

309   [31] N. Moraci, P.S. Calabrò, Heavy metals removal and hydraulic performance in zero-

310   valent iron/pumice permeable reactive barriers, J. Environ. Manag. 91 (2010) 2336–

311   2341.

312   [32] C. Noubactep, S. Caré, F. Togue-Kamga, A. Schöner, P. Woafo, Extending service life

313   of household water filters by mixing metallic iron with sand, Clean – Soil, Air, Water 38

314   (2010), 951–959.

315   [33] Y.B.G. Varma, T. Gopichand, D. Venkateswarlu, Particle size distribution in compacts

316   of solids, J. Chem. Eng. Data 13 (1968) 498–503.

317   [34] A. Felinger, G. Guiochon, Optimization of the experimental conditions and the column

318   design parameters in displacement chromatography, J. Chromatography A609 (1992)

319   35–47.

320   [35] S.I.F. Badawy, M.A. Hussain, Effect of starting material particle size on its

321   agglomeration behavior in high shear wet granulation, AAPS Pharm. Sci. Tech. 5

322   (2004) Article 38 (http://www.aapspharmscitech.org).

323   [36] R.S. Maier, Kroll D.M., R.S. Bernard, S.E. Howington, J.F. Peters, H.T. Davis,

324   Enhanced dispersion in cylindrical packed beds, Phil. Trans. R. Soc. Lond. A 360

325   (2002) 497–506.

326   [37] R.S. Maier, D.M. Kroll, H.T. Davis, Diameter-dependent dispersion in packed cylinders,

327   AIChE Journal 53 (2007), 527–530.

328   [38] S. Comba, A. Di Molfetta, R. Sethi, A comparison between field applications of nano-,

329   micro-, and millimetric zero-valent iron for the remediation of contaminated aquifers,

330   Water Air Soil Pollut. 215 (2011) 595–607.

331   [39] M. Thullner, Comparison of bioclogging effects in saturated porous media within one-

332   and two-dimensional flow systems, Ecol. Eng. 36 (2010) 176–196.

333   [40] A. Wanko, G. Tapia, R. Mosé, C. Gregoire, A new empirical law to accurately predict

334   solute retention capacity within horizontal flow constructed wetlands, Ecol. Eng. 37

335   (2011) 636–643.

336   [41] D. Yuan, L. Zhang, B. Xi, L. He, C. Yan, H. Liu, Design and performance of a filtration–

337   adsorption pool train and drawing water system for small urban recreational water

338   pollution control, Ecol. Eng. 37 (2011) 648–653.

339   [42] A. Brovelli, O. Carranza-Diaz, L. Rossi, D.A. Barry, Design methodology accounting for

340   the effects of porous medium heterogeneity on hydraulic residence time and

341   biodegradation in horizontal subsurface flow constructed wetlands, Ecol. Eng. (2010),

342   doi:10.1016/j.ecoleng.2010.04.031.

343

344

344 **Table 1**: Variability of the operational conditions for column experiments as illustrated by

345 material masses likely to be used in six different columns. D is the internal diameter of the

346 column and L its length. It is assumed that the entire column volume is filled by spherical

347 particle of Fe^0, sand or pumice in an ideal cubic packing (C = 0.64).

348

D	L	V_{column}	V_{solid}	m_{Fe}	m_{sand}	m_{pumice}	Ref.
(cm)	(cm)	(cm^3)	(cm^3)	(kg)	(kg)	(kg)	
2.0	12	37.7	24.1	0.19	0.06	0.015	[27]
2.6	40	212.5	136.0	1.06	0.34	0.087	[28]
4.1	25	330.0	211.0	1.60	0.60	0.135	[29]
5.0	30	589.3	377.1	2.94	0.94	0.241	[30]
5.0	50	982.1	628.6	4.90	1.57	0.402	[31]
5.0	100	1964.3	1257.1	9.81	3.14	0.805	[32]

349
350

351

351 **Table 2**: Relation between the volumetric fraction (α_i) of solid materials in the column (α_{pore}

352 $= 0.36$) and their volumetric percent (P_i) as solid. α_i is obtained by a rule of proportion

353 relative to ($\alpha_{max} = 0.64$ corresponding to 100 % solid). α values are very useful for multi-solid

354 system designs (see text).

P_i	0	10	20	30	40	50	60	70	80	90	100
α_i	0.00	0.064	0.128	0.192	0.256	0.320	0.384	0.448	0.512	0.576	0.640

355

356

356 **Table 3**: selected appropriate solutions for Eq. 11b.
357

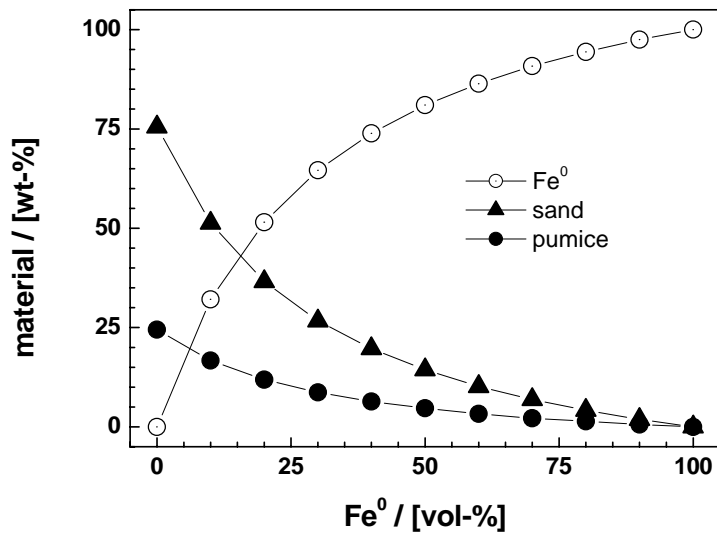|					
α_{quartz}	0.08	0.13	0.16	0.19	0.22
α_{pumice}	0.24	0.19	0.16	0.13	0.1
ϕ_{pumice}	0.33	0.42	0.50	0.62	0.80

358

359

359

360 **Figure 1**: Evolution of the material weight percent in a ternary system Fe^0/sand/pumice as the

361 initial 50:50 sand:pumice mixture (vol) is progressively amended with Fe^0. The sand:pumice

362 volumetric ratio is kept constant during the whole simulation. It is evident that due to

363 difference in densities the weight percent variation is different for individual materials.

364

365

366